Molecular Biology of the Cell
Vol. 6, 1887–1902, December 1995

Domains of Tau Protein, Differential Phosphorylation, and Dynamic Instability of Microtubules

Bernhard Trinczek, Jacek Biernat, Karlheinz Baumann, Eva-Maria Mandelkow, and Eckhard Mandelkow*

Max-Planck-Unit for Structural Molecular Biology, c/o DESY, Notkestrasse 85, D-22603 Hamburg, Germany

Submitted June 22, 1995; Accepted August 31, 1995
Monitoring Editor: Marc W. Kirschner

The dynamic instability of microtubules is thought to be regulated by MAPs and phosphorylation. Here we describe the effect of the neuronal microtubule-associated protein tau by observing the dynamics of single microtubules by video microscopy. We used recombinant tau isoforms and tau mutants, and we phosphorylated tau by the neuronal kinases MARK (affecting the KXGS motifs within tau's repeat domain) and cdk5 (phosphorylating Ser-Pro motifs in the regions flanking the repeats). The variants of tau can be broadly classified into three categories, depending on their potency to affect microtubule dynamics. "Strong" tau variants have four repeats and both flanking regions. "Medium" variants have one to three repeats and both flanking regions. "Weak" variants lack one or both of the flanking regions, or have no repeats; with such constructs, microtubule dynamics is not significantly different from that of pure tubulin. N- or C-terminal tails of tau have no influence on dynamic instability. The two ends of microtubules (plus and minus) showed different activities but analogous behavior. These results are consistent with the "jaws" model of tau where the flanking regions are considered as targeting domains whereas the addition of repeats makes them catalytically active in terms of microtubule stabilization. The dominant changes in the parameters of dynamic instability induced by tau are those in the dissociation rate and in the catastrophe rate (up to 30-fold). Other rates change only moderately or not at all (association rate increased up to twofold, rates of rescue or rapid shrinkage decreased up to ~twofold). The order of repeats has little influence on microtubule dynamics (i.e., repeats can be re-arranged or interchanged), arguing in favor of the "distributed weak binding" model proposed by Butner and Kirschner (1991); however, we confirmed the presence of a "hotspot" of binding potential involving Lys274 and Lys281 observed by Goode and Feinstein, 1994. Phosphorylation of Ser-Pro motifs by cdk5 (mainly Ser 202, 235, and 404) in the flanking regions had a moderate effect on microtubule dynamics while phosphorylation at the "Alzheimer"-site Ser262 by MARK eliminated tau's interactions with microtubules. In both cases the predominant effects of phosphorylation are on the rates of tubulin dissociation and catastrophe whereas the effects on the rates of association or rescue are comparatively small.

INTRODUCTION

The interest in the neuronal microtubule-associated protein (MAP) tau stems mainly from two factors. One is its function as a MAP, specifically a neuronal MAP (Cleveland *et al.*, 1977). MAPs are known to bind to microtubules and to stabilize them, but they may have other functions as well, such as cross-linking to other elements of the cytoskeleton or providing docking sites for enzymes. The combination of such functions probably regulates the behavior of microtubules in

* Corresponding author: Max-Planck-Unit for Structural Molecular Biology, c/o DESY, Notkestrasse 85, D-22603 Hamburg, Germany; email: mand@mpasmb.desy.de

cells, for example their rearrangement during the cell cycle or during neurite outgrowth (for review see Hirokawa, 1994; Kosik and McConlogue, 1994; Schoenfeld and Obar, 1994). MAPs can be diverse, but certain MAPs share common features and probably work by similar mechanisms; this includes the neuronal MAPs tau and MAP2 and the ubiquitous MAP4, which contain three or more internal repeats near their C-termini, flanked by basic and proline-rich regions (Chapin and Bulinski, 1992). All of them are phosphoproteins, and it is thought that signal transduction cascades that initiate cell proliferation or differentiation may control microtubule dynamics via the phosphorylation of MAPs. Thus, the question of how tau interacts with microtubules, and how it is regulated by phosphorylation, is of broad significance even beyond the role of tau in neurons.

A second issue of interest is the role of tau in Alzheimer's disease where it occurs in a pathologically aggregated form (paired helical filaments; PHFs), which are found in the neurofibrillary tangles in the brains of affected individuals. In this state tau is modified in several ways, most prominently by "hyperphosphorylation." This tau protein has lost its ability to stabilize microtubules, and therefore it is believed that microtubule binding, phosphorylation, and aggregation of tau are somehow related to one another (for review see Mandelkow and Mandelkow, 1993; Kosik and Greenberg, 1994).

Several laboratories have addressed these questions by analyzing how different domains of tau (or related MAPs) interact with microtubules, how they are affected by phosphorylation, or how they respond to phosphorylation. There appears to be a consensus that the repeat domain of tau or MAP2 (see Table 1) contributes to microtubule binding and assembly, albeit weakly (Ennulat *et al.*, 1989; Joly *et al.*, 1989), but strong binding requires in addition part of the flanking regions (Kanai *et al.*, 1992; Lee and Rook, 1992). Butner and Kirschner (1991) proposed that the repeat region behaved like a flexible linker because the capacity to bind to microtubules was rather evenly distributed over it; Goode and Feinstein (1994) pointed out that there must be additional "hotspots" that were particularly important for the interaction, such as two lysines between the first and second repeat.

In our own studies we made a number of constructs in which certain domains were removed as cassettes (e.g. repeats, flanking regions, inserts etc.) and assayed their effect on binding to microtubules and on self-assembly. We concluded that the flanking regions behaved like "targeting" domains, important for placing tau on the microtubule surface but not capable of stimulating assembly by themselves, while the repeats acted as "catalytic" domains for self-assembly, but only when embedded in the targeting domains. This led to a "jaws" model of tau's action of microtubules (Gustke *et al.*, 1994). One problem that was not addressed in these studies was the effect of the tau constructs on the dynamic instability of microtubules. This issue seems particularly interesting in the light of recent evidence that many functions of microtubules depend not only on stability as such, but on their ability to perform phase transitions between growth and shrinkage (illustrated by the effect of microtubule poisons on mitosis; Toso *et al.*, 1993). Because neuronal microtubules are also dynamically unstable and regulated by MAPs, we studied the effect of tau on dynamics, and the results are presented here.

To understand the function of MAPs in cells we must understand not only the protein itself, but also how MAPs are regulated by phosphorylation. There seems to be a consensus that phosphorylation is important (for examples see Brugg and Matus, 1991; Verde *et al.*, 1992). However, the reported phosphorylation sites, the kinases or phosphatases, and the magnitudes of the effects can differ considerably. The most obvious role of physiological MAP phosphorylation would be to regulate the interaction with microtubules, although other roles need to be considered as well (e.g. the docking of enzymes; Obar *et al.*, 1989). In the case of tau, an intriguing question is whether and how phosphorylation is involved in its aggregation as paired helical filaments in Alzheimer's disease. In this report we restrict ourselves to the interaction with microtubules, but we use two kinases affecting different phosphorylation sites that are of interest in the context of Alzheimer research. The kinase MARK phosphorylates serine 262, which has a strong effect on microtubule binding (Biernat *et al.*, 1993; Drewes *et al.*, 1995) and may be related to the enhanced phosphorylation of that residue in Alzheimer tau (Hasegawa *et al.*, 1992). The neuronal cdc-like kinase cdk5 phosphorylates Ser-Pro motifs of tau in the regions flanking the repeats (Baumann *et al.*, 1993; Kobayashi *et al.*, 1993; Paudel *et al.*, 1993). This induces the reaction with antibodies that are diagnostic for Alzheimer tau. The phosphorylation pattern of cdk5 overlaps with that of MAP kinase, another proline-directed kinase (Drewes *et al.*, 1992).

The dynamic instability of pure microtubules has been reported by several authors, notably Walker *et al.* (1988), and effects of tau and phosphorylation have been described by Drechsel *et al.* (1992). Several discrepancies exist between these two reports, which we have tried to resolve here. By and large our data confirm those of Walker *et al.* in terms of the parameters of dynamic instability, and the effects of tau are explainable by how it alters rates of dissociation and catastrophe, contrary to the interpretation of Drechsel *et al.*, which placed more importance on the association rates.

MATERIALS AND METHODS

Tubulin and kinases were prepared from porcine brain as described previously (p110^{MARK}, Drewes *et al.*, 1995; cdk5, Baumann *et al.*, 1993). Axonemes were isolated from sea urchin sperm (*Psammechinus miliaris*) according to the method of Bell *et al.* (1982). Human tau cDNA clones were kindly provided by M. Goedert (Goedert *et al.*, 1989), expressed in *Escherichia coli* using variants of the pET vector (Studier *et al.*, 1990), and the proteins were purified, making use of heat stability, Mono S fast performance liquid chromatography, and gel filtration (Biernat *et al.*, 1993; Gustke *et al.*, 1994). Protein concentrations were determined by the BCA method (Smith *et al.*, 1985) using bovine serum albumin as a standard.

Phosphorylation reactions were carried out as described: 50 mM sodium-piperazine-*N*,*N*′-bis(ethansulfonic acid) (PIPES), pH 6.9, 1 mM dithiothreitol, 2 mM EGTA, 6 mM $MgCl_2$, 2 mM ATP, 0.1 mM phenylmethylsulfonyl fluoride, 0.03% Brij-35, 5 μM tau for 2 h at 37°C in the case of p110^{MARK} (Drewes *et al.*, 1995). Under these conditions, MARK (activity 0.1 U/ml) incorporated ≈2 mol P_i/mol tau (mainly Ser262 and Ser356). The activity of cdk5 was 0.014 U/ml (1 U corresponds to the transfer of 1 μmol phosphate per min, using the modified histone H1 peptide PKTPKKAKKL as substrate at 1 mM with 1 mM ATP (see Beaudette *et al.*, 1993). Phosphorylation of tau was done with 0.043 mU of cdk5 and 3.6 μM tau in the same buffer as above in a 30 μl volume for 16 h. The cdk5 incorporated ≈3 P_i (mainly Ser202, Ser235, and Ser404, with minor sites at Ser198, Ser199, Thr205, and Ser400 (see Figure 6). The residues were identified by sequencing of high performance liquid chromatography–purified phosphopeptides (Meyer *et al.*, 1991) and two-dimensional phosphopeptide mapping as described (Drewes *et al.*, 1995).

Microtubule dynamics was assayed by dark field video microscopy as described (Trinczek *et al.*, 1993): 1 μl of tubulin/tau/axoneme mixtures (in 0.1 M Na-PIPES, pH 6.9, 1 mM each of EGTA, dithiothreitol, $MgCl_2$, and GTP) were put on a slide, covered with 18 × 18 mm coverslips, sealed, and warmed up to 37°C in a temperature-controlled air flow within 5 s. Constant temperature of 37°C was maintained by an air flow. Observation started 15 s to 20 min after temperature shift to 37°C, depending on the time needed to find microtubules seeded onto a single axoneme. The experiments were carried out at low axoneme concentration (≈10–100 fM), and at different excess tubulin concentrations so that the polymerized tubulin was negligible compared with the total tubulin concentration (below 5%). This condition was checked microscopically by screening large areas of the preparations for microtubules (1625 dimers/μm and 13 protofilaments). Nucleation activity was directly analyzed by using axoneme-free solutions at 15 μM tubulin and 7.5 μM tau isoforms or constructs simply by counting the number of microtubules per monitor field occurring within 2–3 min after the temperature shift. For each preparation, 10 experiments were performed, and three fields per sample (randomly distributed and separated by time intervals of 20 s) were analyzed, screening the whole range of focal depth. Microtubules were monitored using a Zeiss Axioplan microscope equipped with a Plan-Apochromat 100 ×/1.3 NA oil immersion objective lens, 1.2/1.4 NA oil immersion dark field condenser, and an Osram HBO 100 W/2 mercury lamp. The image was recorded on a AVT-9222 FMK SIT camera (AVT-Horn, Aalen, Germany) connected to a Panasonic SVHS AG 7330 recorder. For each condition ≈20–50 microtubule plus ends and minus ends were analyzed. Data analysis was done as described (Trinczek *et al.*, 1993), following essentially the methods of Walker *et al.* (1988) and the "large scale method" of Gildersleeve *et al.* (1992).

RESULTS

Mechanism of Tau-induced Microtubule Stabilization

The domains of tau are diagrammed in Table 1, along with the constructs used in this study, differing in terms of N-terminal or C-terminal tails, repeats (grey shade), or flanking regions (dark shade). As a reference we first investigated how the full-length four-repeat isoform htau40 (Table 1, top) affects the dynamic state of single microtubule ends, compared with microtubules without tau. PC-tubulin mixed with tau was polymerized onto seeds made from sea urchin sperm in conditions where self-nucleation did not occur, and microtubule dynamics was observed by video microscopy. Examples of life-history plots (length vs. time) are given in Figure 1 for plus ends and minus ends and for different concentrations of htau40, the dependence of rates on tubulin concentration is shown in Figure 2, and deduced rate constants for several tau isoforms and constructs are listed in Table 1, following the analysis of Walker *et al.* (1988).

The growth rates increase linearly with tubulin concentration (Figure 2, A and D), as expected for a bimolecular reaction at microtubule ends. This yields the association rate (corresponding to the slope), dissociation rates (y-intercept), and critical concentration (x-intercept) where association equals dissociation. For example, the values for PC-tubulin without tau are $k_2 = 6.9\ \mu M^{-1}s^{-1}$, $k_{-1} = 32\ s^{-1}$, and $S_{crit} = 4.6\ \mu M$. These and other values are in good agreement with those of Walker *et al.* (1988). Note that the dissociation rate discussed here is the off rate of tubulin subunits during growth, not the (much larger) off-rate during rapid shrinkage.

How does tau affect the rates? Even in the presence of tau, the plots of rate versus tubulin concentration remain linear (Figure 2, A and D). The slope increases, and both intercepts decrease. The association rates increase about twofold for both ends, but the more dramatic effect is the decrease of the dissociation rates (e.g. sixfold at the plus end). This means that the critical concentration drops by an order of magnitude (e.g. 12-fold for plus-ends), down to about 0.4 μM. This confirms earlier reports, derived from bulk assembly measurements, that the main effect of MAPs is to stabilize microtubules against disassembly (Murphy *et al.*, 1977).

In Figure 2, B and E, we compare the mean growth period as a function of tubulin and tau. This parameter is inversely related to the frequency of catastrophe. Mean growth periods increase with tubulin, but the effect is much more pronounced in the presence of tau than without it, rising from about 2 min to over 50 min (a range of f_{cat} from 0.008 s^{-1} to below 0.0003 s^{-1}; Table 2); tau protects against catastrophe much more efficiently than an increase in tubulin. Again a similar behavior is observed at both ends. On the other hand, neither tubulin nor tau have a pronounced effect on the rescue rates (Figure 2, C and F), which range around 0.05 s^{-1} (plus ends) to 0.5 s^{-1} (minus ends). Finally, without tau the rates of rapid shrinkage were ≈1140 and 2110 s^{-1} (for plus and minus ends), de-

Table 1.

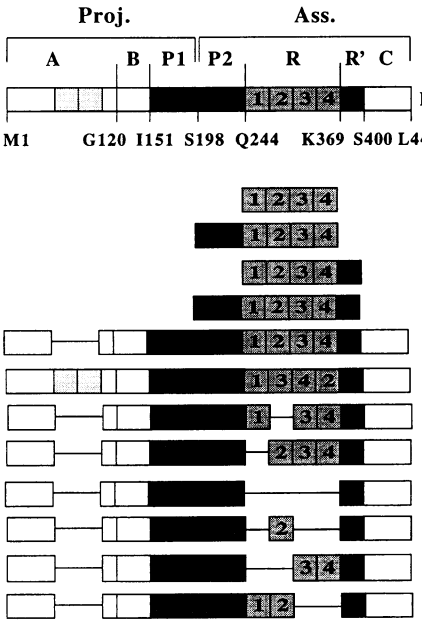

	plus ends			minus ends		
	k_2^e ($s^{-1}\mu M^{-1}$)	k_{-1}^e (s^{-1})	s_c^e (μM)	k_2^e ($s^{-1}\mu M^{-1}$)	k_{-1}^e (s^{-1})	s_c^e (μM)
HT40	14.1(0.8)	5.5(5.3)	0.4(0.4)	8.2(0.4)	6.0(2.8)	0.7(0.4)
K18	7.4(0.5)	41.3(6.4)	5.6(1.2)	4.2(0.4)	25.3(4.4)	6.0(1.0)
K16	8.1(0.7)	39.0(8.8)	4.8(1.5)	4.2(0.1)	21.4(1.6)	5.1(0.5)
K11	9.3(0.6)	25.6(7.4)	2.8(1.0)	4.7(0.4)	15.0(0.5)	3.0(1.3)
K32	10.9(0.4)	2.9(2.8)	0.3(0.3)	6.4(0.3)	1.9(2.6)	0.3(0.4)
HT24	12.0(0.7)	4.0(5.1)	0.3(0.4)	5.8(0.2)	1.8(1.2)	0.3(0.2)
K1342	12.3(0.8)	3.0(5.9)	0.2(0.5)	7.5(0.8)	4.7(5.8)	0.6(0.8)
HT23	12.7(0.7)	38.1(7.8)	3.0(0.8)	6.1(0.8)	19.0(8.6)	3.1(1.8)
K31	10.1(0.4)	21.7(4.0)	2.1(0.4)	5.3(0.6)	14.6(6.2)	2.8(1.2)
K23	9.2(0.6)	30.3(8.6)	3.3(1.2)	4.7(0.2)	17.0(3.0)	3.6(0.8)
K30	12.7(1.1)	42.6(9.9)	3.4(0.8)	6.0(0.5)	20.7(4.3)	3.5(0.8)
K6	13.7(1.6)	50.4(14.5)	3.7(1.1)	6.3(0.3)	23.7(2.6)	3.8(0.5)
K29	12.3(1.6)	29.5(14.6)	2.4(0.6)	6.0(0.9)	18.9(8.8)	3.2(0.8)
PCT	6.9(0.5)	32.0(5.9)	4.6(1.2)	3.3(0.2)	13.7(2.5)	4.2(1.0)

Tau constructs and molecular rate constants of microtubule dynamics. Left, bar diagrams of tau isoforms and constructs. The top shows htau40, the largest isoform in the central nervous tissue (441 residues, all residue numbers refer to this isoform; Goedert *et al.*, 1989). The definition of domains refers to the character of the primary sequence (see Gustke *et al.*, 1994): A, acidic; B, basic; P, proline rich (separated into P1 and P2 at a chymotryptic cleavage site); R, up to four internal repeats of 31 or 32 residues; R', pseudo-repeat; C, C-terminal tail; PROJ and ASS refer to projection and assembly domains. The repeat domain is shaded grey, the flanking domains P and R' are shaded dark. The charges of the domains are as follows (counting D and E as −1, R and K as +1): A, −30 + 6 = −24; B, −4 + 8 = +4; P1, −2 + 7 = +5; P2, −1 + 9 = +8; R1, −2 + 5 = +3; R2, −2 + 5 = +3; R3, −1 + 4 = +3; R4, −5 + 5 = 0; R', −4 + 7 = +3; C, −5 + 2 = −3.

On the right, molecular rate constants for association (k_2^e), dissociation (k_{-1}^e) and critical concentrations of elongation (S_c^e) determined from the plots of growth rates vs. tubulin concentration (compare Figures 2 and 3). Tau/tubulin molar ratio is 1:2 in all cases. PCT is phosphocellulose-purified tubulin preparation without added tau. Standard deviations are shown in parentheses. Shaded fields highlight tau constructs that are particularly efficient in microtubule stabilization, as judged by a low critical concentration (around 0.3 μM) and low dissociation rate constant (around $3s^{-1}$). This category includes only constructs that contain the two flanking regions (P and R', dark shade) and four repeats (R1–R4).

The tau variants in Tables 1 and 2 can be subdivided in three classes of strong, medium, and weak potency to stabilize microtubules (strong values printed in grey boxes). The distinction is based on the "dissociation" parameters (dissociation rate, catastrophe rate, and critical concentration). Strong: $K_{-1} \approx 3$–$4\ s^{-1}$, $S_c \approx 0.3\ \mu M$, 1/cat ≈50–60 min. Includes constructs with four repeats and both flanking domains (htau24, htau40, K1342, and K32). Medium: $k_{-1} \approx 20$–$50\ s^{-1}$, $S_c \approx 2$–$4\ \mu M$, 1/cat ≈8–20 min. Includes constructs with at least one repeat and both flanking domains (htau23, K31, K30, K6, and K29). Weak: $K_{-1} \approx 25$–$40\ s^{-1}$, $S_c \approx 3$–$6\ \mu M$, 1/cat ≈2–4 min. Includes constructs with no repeat (K23), no flanking region (K18), or only one flank (K16 and K11). These constructs are equivalent to "no tau" (pure tubulin and PCT).

creasing about twofold to 650 and 890 s^{-1} at high tau/tubulin ratios (1:1). In summary, the effect of tau on parameters related to growth (growth rate and rescue) is visible but moderate, whereas there is a very pronounced protection against disassembly, as revealed by lower off-rates, lower critical concentrations, and fewer catastrophes.

Effects of Tau Domains on Microtubule Dynamics

The above experiments provided the yardstick for comparing the different tau constructs whose parameters are listed in Tables 1 and 2. The experiments of Table 2 were done at tau:tubulin ratios of 1:2 because this is the stoichiometry at saturation for most constructs (see Gustke *et al.*, 1994), and the effects on dynamic instability are most apparent. Representative curves of growth rate versus tubulin concentration are shown in Figure 3.

Core Domains Versus Tails. We can broadly distinguish the core domains (repeats and flanking regions) shown in grey or dark shades in the diagrams (e.g. Table 1), and the lightly or unshaded tails (N- or C-terminal). As long as the core domains are present,

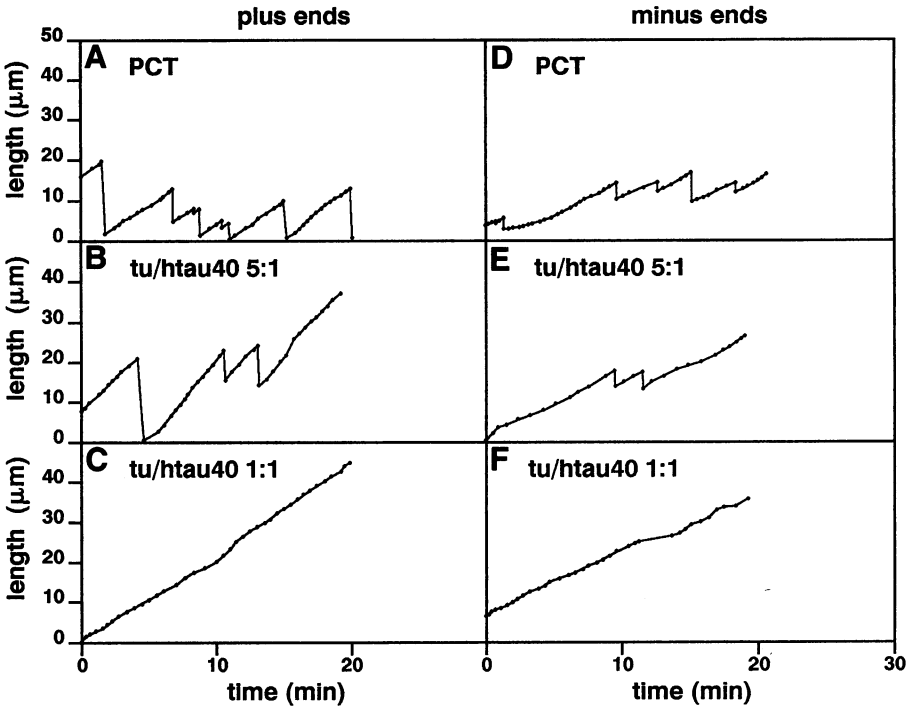

Figure 1. Life history plots (length vs time) of microtubules seeded onto axonemes. Left, plus ends; right, minus ends. (A and D) Tubulin without tau (control, 15 μM tubulin). (B and E) 15 μM tubulin, 3 μM htau40. (C and F) 5.5 μM tubulin, 5.5 μM htau40. The most notable effect of added tau is to suppress catastrophes.

variations in the tails appear to be of minor importance (compare htau24 and K32 in Table 1). We can therefore disregard them in our present context; this also applies to the two inserts near the N-terminus (in agreement with our earlier binding studies).

The Repeat Motif. We first asked whether the number of repeats mattered for dynamic instability. This is clearly the case: when comparing the "fetal" isoform htau23 containing 3 repeats with 4-repeat isoforms (e.g. htau24) there is a parallel shift in the growth versus concentration plot (Figure 3A), indicating that the two isoforms correspond to similar association constants but to very different dissociation constants; this in turn leads to a 10-fold higher critical concentration (≈3 μM), approaching that of tau-free microtubules (4.6 μM). Removing other repeats (e.g. R1, as in K31), or removing more than one repeat (K23, K30, K6, and K29) leads to similar results. We conclude that four repeats are required to obtain a good protection against disassembly (low dissociation rate and low frequency of catastrophe). The parameters of these constructs are shown in shaded areas in Tables 1 and 2 (K32, htau40, K1342, and htau24).

Secondly, we asked whether the order of repeats mattered. This was prompted by the observation of Goode and Feinstein (1994) that the inter-repeat region between R1 and R2 contained a hotspot of binding activity. We removed R2 and placed it behind R4, creating construct K1342. There was no significant change in parameters, i.e., the construct behaved similar to other 4-repeat constructs (but see below). Similarly, connecting the flanking regions with the repeats in different ways has only a moderate effect on dynamic instability (Figure 3C); the number of repeats (four vs. less than four) is clearly more important than their sequence (compare K31, K30, K6, and K29).

Repeats Versus Flanking Regions. The repeats are often considered as the microtubule-binding domain. However, this is an oversimplification because the repeats alone bind very weakly whereas repeat-less tau binds strongly. The discrepancy can be resolved by considering the repeats as catalytic domains in combination with the flanking regions as targeting domains (the jaws model; Gustke *et al.*, 1994). This concept explains the effects on dynamic instability as well (Figure 3B): the repeats alone (K18), or the repeats with only one flanking region (K16 and K11) show parameters that approach those of tau-free microtubules, i.e., high critical concentration, high dissociation rate, and frequent catastrophes. However, when the repeats are combined with both flanking regions, as in K32, the dissociation rate becomes small, and microtubules become protected against catastrophes (mean growth periods in excess of 60 min; Table 2).

The tau constructs considered up to this point allow one to classify them broadly into three groups, depending on how potently they stabilize microtubules (listed in Table 1). "Strong" constructs have low dissociation constants (≈3 s^{-1}), low critical concentrations (≈0.3 μM), and low catastrophe rates or long

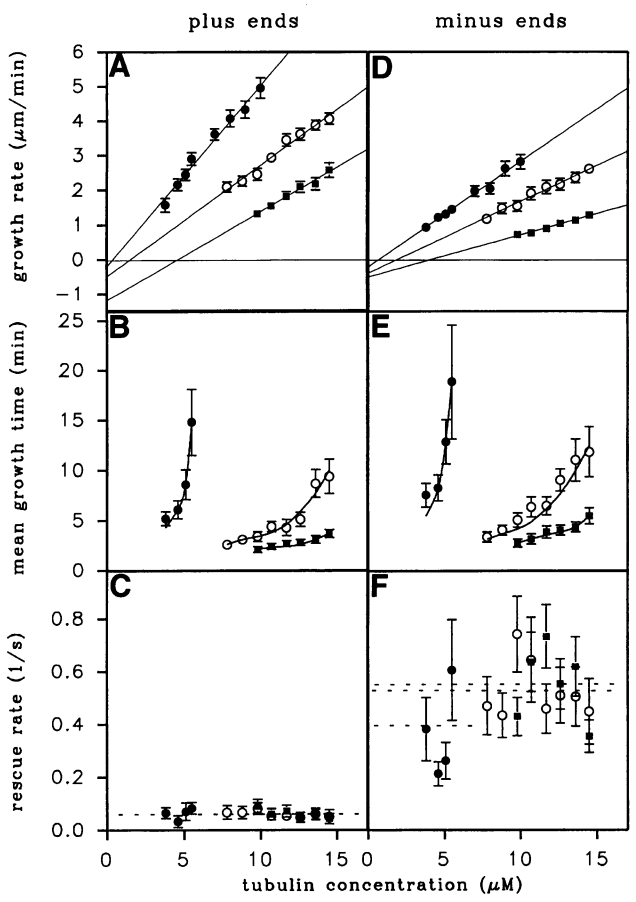

Figure 2. Rate of elongation (A and D), mean growth time (B and E), and rescue frequency (C and F) of microtubules as a function of tubulin concentration in the presence of tau (htau40 isoform). Pure tubulin (filled squares); tubulin/tau, 5:1 (open circles); tubulin/tau, 1:1 (filled circles). Left, plus ends (A–C); right, minus ends (D–F). The slopes in panels A and D are proportional to the association rates of tubulin·GTP (TuT), the extrapolated y-intercepts to the dissociation rates of tubulin during the growth phase, and the x-intercepts to the critical concentrations of elongation. For both ends the critical concentration of elongation decreases with increasing amounts of added htau40. This is due to a strongly reduced dissociation rate as well as to a slightly increased association rate of tubulin at growing microtubule ends. The decrease in critical concentrations of elongation (k_{-1}^e/k_2^e) correlates with increasing mean growth times (decreasing rates of catastrophe; B and E) in the presence of tau. By contrast, rescue frequencies show little change within the concentration range analyzed, and within the resolution limits of the microscope (C and F, dashed lines). The differences between plus and minus ends are observed at all tau concentrations, with minus ends having significantly higher rescue frequencies than plus ends. Error bars in panels A and D, SEM; error bars in B, C, E, and F, $1/\sqrt{n}$. For data points without an error bar, the values range within the symbol size.

growth periods (≈50 min). This includes constructs or isoforms with four repeats and both flanking regions. "Medium" strength constructs are characterized by higher rates of dissociation and catastrophe; they include constructs with both flanking regions, but less than four repeats (one, two, or three). Finally, "weak" constructs have even higher rates of dissociation and catastrophe, to the point where they have no appreciable effect compared with tubulin alone. This includes constructs with only one or no flanking region, repeat-less tau (K23), or repeats only (K18). Note that the classification is based on the dissociation parameters k_{-1} and catastrophe, whereas association constants, rescue rates, or rapid shrinkage show relatively little variation.

Microtubule Self-nucleation. So far we have considered microtubules assembled onto flagellar axonemes as templates because we wanted to observe growth or shrinkage independently of self-nucleation of microtubules. The next question was how nucleation would depend on tau constructs. This was assayed by mixing tubulin and tau in a fixed ratio (2:1) and observing the number concentration of microtubules formed. As seen in the histogram of Figure 4, the tau constructs can be broadly subdivided into three classes, strong, medium, and weak nucleators (>200, around 100, and <20 microtubules per field, respectively), and this classification coincides with the one described above: strong nucleators contain both flanking domains and all four repeats (htau40, htau24, K32, and K1342); medium nucleators contain both flanking domains and at least one repeat (htau23, K31, K30, K6, and K29), and weak nucleators contain either no repeat (K23) or only one or none of the flanking regions (K16, K11, and K18). In other words, the same properties of tau that govern the dissociation rate and the frequency of catastrophes appear to govern nucleation as well, suggesting that tau functions mainly by preventing the nucleating tubulin subunits from falling apart, more than by promoting their association.

Hotspots of Assembly Activity. Goode and Feinstein (1994) reported that two lysines near the boundary of repeats 1 and 2 were particularly effective in promoting microtubule assembly (Lys265 and Lys272 in the rat tau sequence, corresponding to Lys274 and Lys281 in human tau). We designed two constructs to test whether this result was applicable to dynamic instability as well. In the first experiment, the second repeat was removed and placed behind repeat 4 (K1342; see Figure 5). This disrupts the R1-R2 boundary; in terms of net charge the basic repeat R2 (charge +3) is put in the position of the neutral repeat (R4). However, as mentioned above, there was no significant change in any of the rate constants (see Tables 1 and 2). This could be interpreted to mean that the locations of these two lysines are not important for the interaction with microtubules. This picture changed with the second experiment, in which the two lysines were replaced by alanines (mutant Ala274/Ala281). With this mutant the frequency of catastrophes increased more

Table 2.

Tau isoforms and constructs		Tu/Tau-conc.	plus ends		minus ends	
			v^e	1/cat	v^e	1/cat
strong nucleators		(μM)	(μm/min)	(min)	(μm/min)	(min)
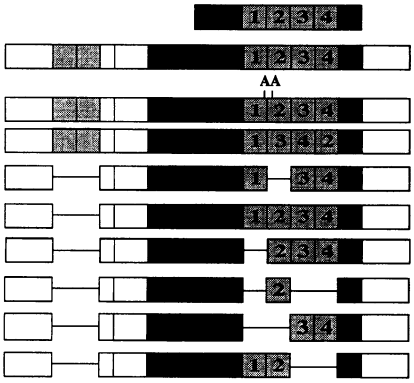	K32	7/3.5	2.7(0.4)	62.1[34]	1.8(0.3)	50.4[41]
	HT40	7/3.5	2.8(0.6)	57.2[44]	1.6(0.4)	51.7[52]
	A274/281	7/3.5	1.9(0.4)	9.6[104]	0.9(0.2)	10.5[53]
	K1342	7/3.5	3.2(0.5)	60.0[30]	1.5(0.3)	41.8[35]
	HT23	7/3.5	1.8(0.6)	18.2[61]	1.1(0.3)	15.2[47]
	HT24	7/3.5	2.9(0.5)	66.3[29]	1.7(0.3)	44.8[47]
	K31	7/3.5	1.9(0.4)	17.2[76]	0.9(0.2)	12.3[56]
	K30	7/3.5	1.9(0.4)	8.5[89]	1.0(0.2)	12.2[58]
	K6	7/3.5	1.8(0.4)	9.0[63]	0.8(0.2)	14.3[42]
	K29	7/3.5	2.5(0.6)	13.5[45]	1.1(0.2)	11.8[40]
weak nucleators						
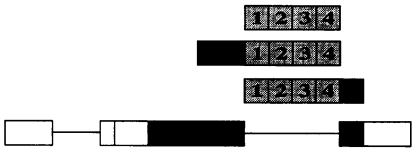	K18	11/5.5	1.6(0.3)	2.1[30]	0.7(0.2)	2.7[39]
	K16	11/5.5	1.8(0.3)	2.7[47]	0.9(0.2)	4.0[28]
	K11	11/5.5	2.7(0.2)	4.2[34]	1.3(0.2)	5.5[20]
	K23	8/4	1.5(0.5)	2.8[70]	0.7(0.3)	5.6[50]
	PCT	10	1.3(0.3)	2.0[64]	0.7(0.1)	2.8[44]
HT40 phosphorylated						
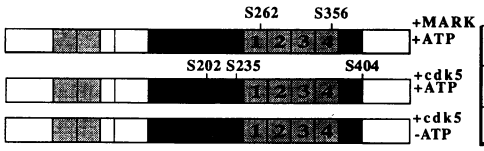	+MARK +ATP	10/5	1.3(0.4)	1.8[86]	0.6(0.1)	2.2[65]
	+cdk5 +ATP	7/3.5	1.6(0.3)	17.1[52]	0.8(0.2)	14.7[48]
	+cdk5 -ATP	7/3.5	2.8(0.7)	60.9[97]	1.5(0.4)	68.4[49]

Rates of growth (v^e) and mean growth periods t^e (reciprocal of the rate of catastrophe, k^{cat}) of microtubule plus and minus ends. Left, diagram of tau isoforms or constructs. The molar ratio of tubulin:tau was kept constant at 2:1 (e.g. 7 μM/3.5 μM, see first column). Parentheses indicate standard deviations and brackets indicate number of transitions measured. Values for strong constructs are shown shaded; they correspond to long growth periods or low catastrophe rates. Note that strong constructs are also good nucleators (see Figure 4); weak constructs (and nucleators) are grouped together in the middle box. The group at the bottom illustrates the effect of phosphorylation of htau40 by MARK and cdk5 (with ATP, or without ATP as control). Phosphorylation by cdk5 makes htau40 medium and MARK makes it weak.

than sixfold, or mean growth times dropped from 60 min down to 10 min (Table 2 and Figure 5), moving the construct from the strong class into the medium class of stabilizers. This confirms the results of Goode and Feinstein and illustrates that individual residues could be important, even when entire blocks or residues are exchangeable.

Effects of Phosphorylation of Tau. The interaction of tau with microtubules is thought to be regulated by phosphorylation, but the phosphorylation sites involved are not well characterized, partly because a number of kinases can phosphorylate tau at different sites. Two types of phosphorylation sites appear to be particularly interesting. One comprises the Ser-Pro or Thr-Pro sites, clustered mainly in the two domains flanking the repeats, which can be phosphorylated by several proline-directed kinases (e.g. MAP kinase or cdk5; for review see Mandelkow and Mandelkow, 1993) and generate epitopes characteristic of Alzheimer tau. The others are the serines in the four KXGS motifs within the repeats, phosphorylated by the kinase p110 MARK. With regard to microtubule binding, we reported earlier that even extensive phosphorylation by proline-directed kinases has only a moderate effect (≈20%), whereas the phosphorylation

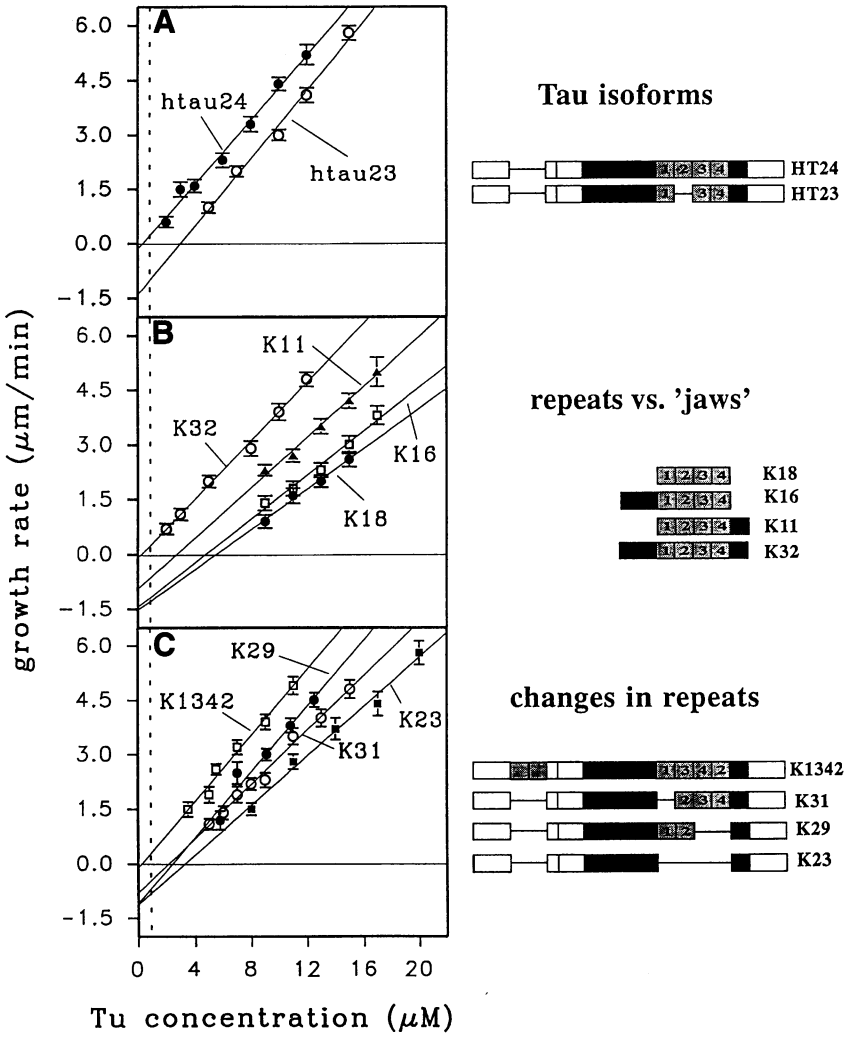

Figure 3. Growth rates of axoneme-seeded microtubule plus ends as a function of tubulin concentration for tubulin preparations with different tau isoforms (A, htau23 and htau24) and tau constructs K18, K16, K11, and K32 (B), and K23, K31, K29, and K1342 (C). Molar ratio of tubulin/tau mixtures is 2:1 in all cases. Right, bar diagrams of added tau protein. The rate constants determined from the plots are summarized in Table 1. Note that there is little variation in association rates (similar slopes); the main differences are in the dissociation rates (y-intercepts) and critical concentrations (x-intercepts).

of Ser262 (in the first KXGS motif) has a dramatic effect on the affinity of tau to microtubules (Biernat *et al.*, 1993; Drewes *et al.*, 1995).

To test how these types of phosphorylation affect dynamic instability we phosphorylated tau either in the repeats with MARK, or in the flanking regions with cdk5, using protocols described previously (Baumann *et al.*, 1993; Drewes *et al.*, 1995). MARK incorporated about 2 P_i (mainly at Ser262 and Ser356, the latter being of secondary importance for microtubule binding; Drewes *et al.*, 1995), cdk5 incorporated about 3 P_i (mainly Ser202, Ser235, and Ser404, with lesser phosphorylation at Ser198, Ser199, Thr205, and Ser400; Figure 6). In conditions where unphosphorylated tau supported steady growth of microtubules (Figure 7A, top trace), cdk5 increased the rate of catastrophe about fourfold, and MARK increased it even 40-fold (Figure 7C; Table 2, bottom). As before, the effect on growth rate was relatively small (twofold). Thus, in our classification scheme tau phosphorylated by cdk5 would be medium, while tau phosphorylated by MARK becomes weak, equivalent to no tau at all (compare values with PC-tubulin in Table 2). These results confirm the earlier binding studies, i.e., proline-directed phosphorylation has a moderate effect and phosphorylation of Ser262 has a large effect on microtubule dynamics.

DISCUSSION

MAPs and Microtubule Dynamic Instability

Microtubules establish and rearrange themselves by virtue of their self-assembly and dynamic instability. MAPs and their phosphorylation are thought to be important regulators of microtubule dynamics; well-studied examples are those of mitosis and neurite outgrowth (for reviews see Kosik and McConlogue,

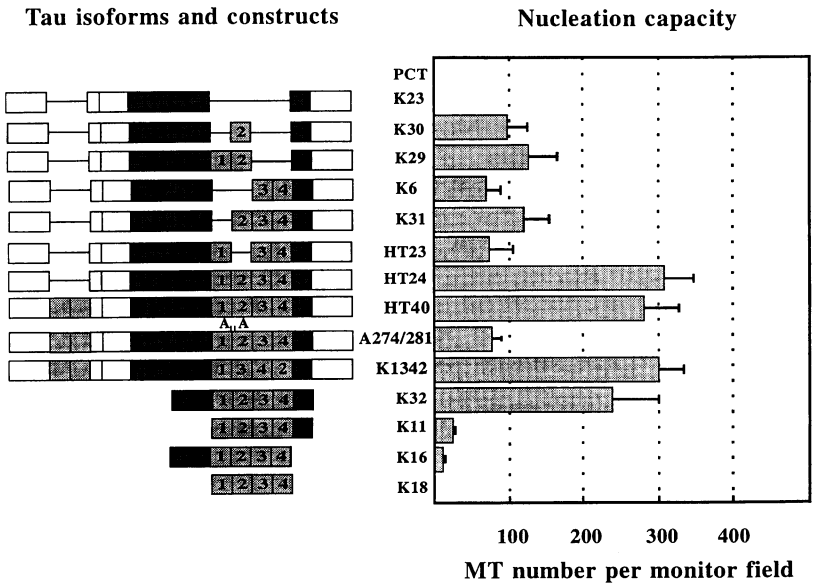

Figure 4. Histogram showing the efficiency of microtubule nucleation in the presence of different tau constructs. Tubulin concentration was 15 μM and that of tau was 7.5 μM in all cases. The classification into strong, medium, and weak constructs, derived from the dynamic instability parameters (Tables 1 and 2) applies to nucleation as well, i.e., strong constructs are also strong nucleators. Note that repeat-less tau (K23) does not nucleate microtubules even though it binds tightly to microtubules. The lysine mutant A274/A281 converts htau40 from strong to medium. N- or C-terminal tails have no influence on nucleation (compare htau24 and K32).

1994; Schoenfeld and Obar, 1994). There seems to be a consensus that MAPs stabilize microtubules, and that the phosphorylation of MAPs weakens their stabilizing effect. On a molecular level, one would therefore like to know what domains of MAPs determine microtubule dynamics, which parameters of dynamics are affected, what phosphorylation sites influence the stability, what kinases or phosphatases regulate them, and so on.

Earlier studies of MAP-microtubule interactions were mostly performed in bulk solution. One important result was that MAPs stabilize microtubules by lowering the dissociation rate of subunits, rather than increasing the association rate (Murphy *et al.*, 1977). More recently, with the advent of video microscopy techniques and the concept of dynamic instability, most authors turned to the study of single microtubules because this provides a more detailed picture of microtubule behavior. For each end (plus or minus) one can observe five independent parameters as follows: 1) association and 2) dissociation rate constants during elongation, k_2 and k_{-1}, derived from a plot of growth rate versus tubulin concentration (this also yields the critical subunit concentration, $S_c = k_{-1}/k_2$); 3) dissociation rate during rapid shrinkage (k_{shr}); and 4) rate of catastrophe and 5) rate of rescue (or their reciprocals, the mean duration of growth and shrinkage). Several reports on different aspects of dynamic instability have appeared so far and are as follows: the dynamics of microtubules made of pure tubulin (Horio and Hotani, 1986; Walker *et al.*, 1988; Gildersleeve *et al.*, 1992; Trinczek *et al.*, 1993; Vandecan-

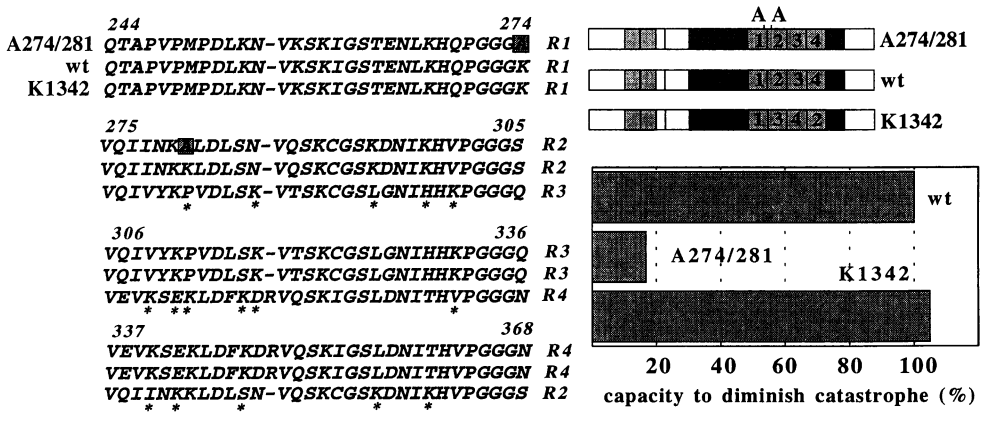

Figure 5. Residues in the four repeats (wild type, middle row), lysine mutations A274/A281 (top row), and domain exchange mutant K1342 (2nd repeat behind fourth, bottom row). The effects on the frequency of catastrophe are diagrammed on the right. For K1342, those residue positions are underlined that mismatch the wild-type lysine residue distribution. In the wild type the net charge of the repeats is +3, +3, +3, and 0; in the mutant K1342 the sequence is +3, +3, 0, and +3; and in the double lysine mutant it is +2, +2, +3, and 0. In the mutant K1342 there is a major rearrangement of the net charges, which has, however, no effect on microtubule dynamics; this is in contrast to the lysine mutant even though the change seems minor in terms of overall charge distribution.

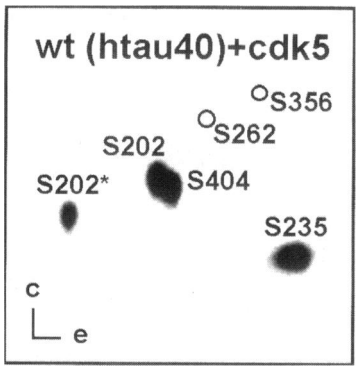

Figure 6. Tryptic phosphopeptide map obtained by 2D TLE/TLC of htau40 phosphorylated with cdk5 (derived from the same preparation that was also used for dark field microscopy). About 3 P_i were incorporated, and the major sites were Ser202, Ser235, and Ser404 as indicated. The spot marked S202* contains doubly phosphorylated peptides, Ser202 in combination with either Ser198, Ser199, or Thr205, as determined by phosphopeptide sequencing. The spot marked S202 contains a ≈20% contribution from the same peptide phosphorylated at Ser198. The spot marked S404 contains an ≈30% contribution from the same peptide phosphorylated at Ser400. Note that phosphopeptides corresponding to phosphorylation of the repeat domain did not occur. For comparison, the circles indicate the positions of phosphopeptides containing Ser262 and Ser356 phosphorylated by MARK (see Drewes *et al.*, 1995). Vertical dimension, c = chromatography; horizontal dimension, e = electrophoresis.

delaere *et al.*, 1995); the effects of MAPs (Drechsel *et al.*, 1992 for tau; Pryer *et al.*, 1992 for tau and MAP2; Kowalski and Williams, 1993 for MAP2; Itoh and Hotani, 1994 for MAP2; and the effects of MAP phosphorylation (Drechsel *et al.*, 1992, Brandt *et al.*, 1994, and Drewes *et al.*, 1995 for tau; Ookata *et al.*, 1995 for MAP4). Several authors have observed microtubule dynamics cell extracts containing nucleation centers (centrosomes), different kinases, and different MAPs (e.g. Bre and Karsenti, 1990; Verde *et al.*, 1992; Andersen *et al.*, 1994). Finally, dynamic instability has been observed directly in cells (Cassimeris *et al.*, 1988; Sammak and Borisy, 1988; Schulze and Kirschner, 1988; Belmont *et al.*, 1990; Shelden and Wadsworth, 1993; Dhamodaran and Wadsworth, 1995). Studies pertinent to our discussion also include those where the binding of MAPs or MAP domains to microtubules was assayed, e.g. for tau (Ennulat *et al.*, 1989; Butner and Kirschner, 1991; Lee and Rook, 1992; Goode and Feinstein, 1994; Gustke *et al.*, 1994); for MAP2 (Joly *et al.*, 1989; Coffey and Purich, 1995); or for MAP4 (Aizawa *et al.*, 1991, Ookata *et al.*, 1995, Olsen *et al.*, 1995).

Considering this body of data it is notable that, beyond the consensus that MAPs somehow stabilize microtubules, there is little agreement in detail. Some authors see the main effect of MAPs in the association parameters, others see the effect mainly in dissociation parameters. The discrepancies may be explained in part by differences in protein preparations or other experimental procedures, but even so the situation is unsatisfactory at present. To quote some examples, Salmon and colleagues (Walker *et al.* 1988; Pryer *et al.* 1992) argue that MAPs act to prevent dissociation of tubulin, while Drechsel *et al.* (1992) see the main effect in association parameters. Reported dissociation constants between tau and microtubules range from 0.1 μM to above 10 μM (Ennulat *et al.*, 1989; Butner and Kirschner, 1991; Goode and Feinstein, 1994; Gustke *et al.*, 1994). Finally, a general difficulty is that the dynamic instability observed in vitro does not necessarily explain the situation in cells where growth rates and dynamics can be unexpectedly high (Cassimeris *et al.*, 1988; Belmont *et al.*, 1990; Shelden and Wadsworth, 1993). Regarding MAP phosphorylation, apart from the consensus that this tends to destabilize microtu-

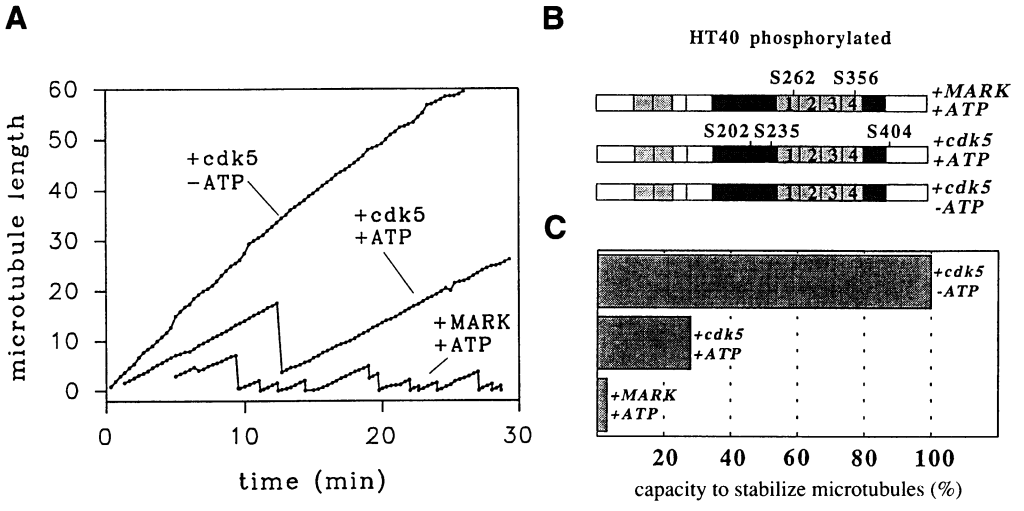

Figure 7. Effect of differentially phosphorylated tau protein on microtubule dynamics. On the left (A), life history plots of microtubule plus ends in preparations containing 7 μM tubulin and 3.5 μM tau40 phosphorylated with cdk5 or MARK (with ATP or without as a control). Upper right (B), bar diagrams of htau40 with the main phosphorylation sites. Lower right (C), histogram showing the relative catastrophe-regulating activities of htau40 phosphorylated either by cdk5 (middle bar) or MARK (bottom), and compared with the control without ATP (= 100%). Compare with Table 2.

bules, there is a similar lack of agreement on the phosphorylation sites, their importance for microtubule dynamics, and the kinases involved; this issue is complicated by the multitude of potential phosphorylation sites (the complexity was well illustrated for MAP2 by Brugg and Matus, 1991).

In this situation it is clear that more data are required to explain the regulation of microtubule dynamics via MAPs, and that it may be premature to hope for a unifying mechanism. In the present study, our approach has been to construct tau proteins where the domains were varied as cassettes and to monitor their effect on microtubules by video microscopy. This allowed us to compare the data with those of tau-microtubule binding studies and bulk assembly properties (e.g. Gustke *et al.*, 1994). In addition we have used kinases with well-characterized phosphorylation sites to determine the effect of tau phosphorylation on microtubule dynamics. Most of the rates we observe for MAP-free microtubules are in very good agreement with those of Salmon and colleagues, and the same holds qualitatively for the effects of MAPs (i.e., a reduction mainly in the disassembly parameters; cf. Walker *et al.*, 1988; Pryer *et al.*, 1992). In particular, similar to these authors, we observe a measurable critical concentration in the μM range that is sensitive to MAPs and phosphorylation (in contrast to Drechsel *et al.*, 1992).

Tau Domains and Dynamic Instability

One novel aspect of the data is that the potency of tau's domains with respect to microtubule dynamics can be classified as strong, medium, and weak (strong ones are shaded in Tables 1 and 2). Most observable parameters are influenced to some extent, but the important ones are the dissociation rate constant k_{-1} (varying from 3 s^{-1} to 50 s^{-1} for microtubule plus ends) and the catastrophe frequency or mean growth time (varying from 2–60 min in our conditions). Because the association rate constant k_2 shows little variation (around 10 $\mu M^{-1}s^{-1}$), the range in dissociation rates translates into a range of critical tubulin concentrations between 0.2 and 5 μM (Table 1). These rate constants refer to the elongation process and reflect the ability of tubulin·GTP to associate and dissociate from a microtubule end. Rapid shrinkage (presumably by loss of tubulin·GDP) is much faster ($\approx$1000s^{-1}), but is only moderately affected by tau (up to twofold). The ability of tau to support microtubule self-nucleation follows the same classification, i.e., strong nucleation appears to be related to a low dissociation rate and rare catastrophe.

Strong constructs and isoforms include those that contain the two flanking domains and four repeats; the prototype is full-length tau (htau40). Constructs with only one to three repeats have a medium potency, for example the juvenile isoform htau23 (three repeats). Weak constructs behave almost as if they were not present at all, i.e., their dynamic instability parameters are very similar to those of MAP-free microtubules. Weak constructs include those that have either no repeat (as repeat-less tau, K23), or only one or none of the flanking regions, e.g. K18, a repeat-only construct. Tau's effects on microtubule dynamics can essentially be traced back to the repeats and the flanking regions P and R′, whereas the N- and C-terminal tails appear to be of secondary or no importance (but may influence other effects such as bundle formation).

The results on dynamic instability are in good agreement with our earlier studies on microtubule binding and bulk assembly (Gustke *et al.*, 1994). In fact the present classification scheme is also applicable to the dissociation constants reported earlier. Strong constructs have K_d values around 1–2 μM, medium constructs tend to bind somewhat more weakly ($K_d \approx$2–5 μM, a difference that was not considered very important at the time), while weak constants had clearly higher values (10 μM and up). Thus a weak effect on microtubule dynamics implies weak binding. Note, however, that the converse does not hold: there are constructs such as the repeatless tau (K23) that can bind tightly to microtubules but have no potency to influence dynamics. This has lead us to propose a jaws model of tau-microtubule interactions: the flanking regions are the targeting domains that position tau on the microtubule surface, but the "glue" for keeping tubulin subunits and protofilaments together comes from the repeats, even though they bind only weakly by themselves.

Although the number of repeats is important for microtubule dynamics (four being the most potent), their order seems not to matter much; one can change the connection between flanking regions and repeats, and one can even swap entire repeats, without a major effect. This is well illustrated by construct K1342 where the charge distribution of the repeats is altered by swapping. This would argue in favor of Butner and Kirschner's (1991) model of a distributed weak binding function spread out over the region of repeats. However, this does not exclude the possibility that certain residues are of particular importance for the tau-microtubule interaction. For example, the two lysines 274 and 281 make an unusually large contribution, in agreement with the results of Goode and Feinstein (1994).

Given these observations it is tempting to speculate on the structural basis of the tau-tubulin interaction. Because microtubules have repeating subunits, and because tau has internal repeats, it seems natural to assume that different tau repeats bind to different subunits in the microtubule lattice. However, there are

several difficulties with that assumption that can be summarized as follows: tau binds well to microtubules even without the repeats (Gustke *et al.*, 1994), the binding potential is largely delocalized over the sequence (Butner and Kirschner, 1991), and the internal structure of tau resembles that of a random coil, without secondary structure elements that are usually the hallmarks of repetitive binding sites (Schweers *et al.*, 1994). As an alternative it may be worth considering the repeats as elements required to stabilize a conformation of tau that is competent to interact with microtubules. To quote an analogous example, peptides derived from the α-helical rod domain of intermediate filaments are not necessarily α-helical by themselves, unless they become properly embedded within other domains of the same molecule or neighboring ones (Geisler *et al.*, 1993). We know, for example, that 4-repeat tau is folded such that the cysteines 291 and 322 in repeats 2 and 3 are in close proximity in solution and can easily be cross-linked into intramolecular disulfides. In 3-repeat tau the second repeat is absent, presumably leading to a different conformation of the remaining repeats (this is well illustrated by the fact that oxidized 3-repeat tau constructs readily dimerize and assemble into fibers similar to Alzheimer PHFs; Schweers *et al.*, 1995). Additional evidence for a folded conformation comes from antibodies that react with either of the flanking domains, as long as two or more repeats are present (Lichtenberg *et al.*, 1992). The same difference in conformation could account for the difference between strong and medium, or weak interactions with tubulin.

Another notable point is that the interaction of tau with microtubules is restricted to positively charged domains, proline-rich (P), repeats (R), and pseudo-repeat (R′) (see legend to Table 1). These domains reinforce bonding, while the others are either neutral (e.g. most of the projection domain) or anti bonding. The effect is particularly visible for the acidic C-terminal tail (roughly the final 40 residues), which is antagonistic to tau-microtubule binding (Gustke *et al.*, 1994). It is instructive to compare this with MAP4 where the acidic tail includes the flanking region corresponding to R′, and therefore the whole region downstream of the repeats becomes anti-bonding (Olson *et al.*, 1995). The basic nature of the tau domains and the acidic nature of tubulin's C-terminal region are suggestive of a largely electrostatic interaction that would be weakened by the phosphorylation of tau.

Tau Phosphorylation and Dynamic Instability

Tau, like most MAPs, is a phosphoprotein, it is probably regulated in its physiological state, and it is hyperphosphorylated in Alzheimer's disease. A key problem is therefore to find out how phosphorylation changes the properties of tau. This breaks down into two parts: How does phosphorylation change the interaction between tau and microtubules? And secondly, how does phosphorylation influence tau's aggregation into Alzheimer-paired helical filaments? In this report we deal only with the first question. A number of papers have appeared on the issue, describing phosphorylation sites, kinases, and effects on microtubules. For the present purpose it is useful to distinguish three kinds of phosphorylation sites and corresponding cases: 1) some sites are affected by second-messenger dependent kinases such as PKA, PKC, CaMK, and others (e.g. Ser214, 324, 356, 409, and 416 by PKA; Ser214, 324, and Thr 377 by PKC; Ser416 by CaMK [Steiner *et al.*, 1990; Correas *et al.*, 1992; Scott *et al.*, 1993; for a summary see Drewes *et al.*, 1995]). 2) Ser-Pro or Thr-Pro sites, mostly in the flanking regions, are affected by several proline-directed kinases (MAP kinase, Drewes *et al.*, 1992; GSK-3, Hanger *et al.*, 1992 and Mandelkow *et al.*, 1992; cdk5, Paudel *et al.*, 1993, Baumann *et al.*, 1993, and Kobayashi *et al.*, 1993; other proline-directed kinases, Ishiguro *et al.*, 1991, Ledesma *et al.*, 1992, and Vulliet *et al.*, 1992). These kinases are of interest in Alzheimer's research because the phosphorylated epitopes can be diagnostic of Alzheimer tau (reviewed in Mandelkow and Mandelkow, 1993; Kosik and Greenberg, 1994). Independently of that, proline-directed kinases are involved in the transduction of extracellular signals to the cell's interior, and thus would provide a pathway whereby MAPs and microtubules could be rearranged. 3) There are kinases that phosphorylate Ser262 in the first KXGS motif, such as MARK. This residue is important because it shows increased phosphorylation in Alzheimer tau (Hasegawa *et al.*, 1992; Gross *et al.*, 1994), and it affects the tau-microtubule interaction in a unique manner (Biernat *et al.*, 1993; Drewes *et al.*, 1995).

In this report we are mainly concerned with the second and third categories mentioned above because this allows one to distinguish the effects of phosphorylation within the repeats and in the flanking regions, and because in our hands the phosphorylation by PKA, PKC, etc. had little effect on the binding of tau to microtubules. In earlier binding studies involving phosphorylation of the flanking regions by MAP kinase we had found a reduction in binding of about 20%, i.e. only a moderate effect, compared with the phosphorylation of Ser262 (Biernat *et al.*, 1993). This is now confirmed in terms of dynamic instability parameters. We used the kinase cdk5 (whose phosphorylation pattern overlaps with that of MAP kinase; in the present experiments there were three main sites at Ser202, Ser235, and Ser404, all followed by a Pro). The most noticeable effect was on the catastrophe whose frequency increased fourfold, which places the cdk5-phosphorylated tau in the class of medium potency. Although the effect of cdk5 is noticeable, it is dwarfed by the much larger effect of phosphorylation by

MARK (10 times larger than that of cdk5; Figure 7). The data are consistent with the earlier binding studies in that the phosphorylation of the flanking regions has a modulatory effect on the interaction between tau and microtubules, but the phosphorylation of the repeats, specifically Ser262, is the one that can eliminate tau's interactions altogether. In the context of tau's structure discussed above, this effect highlights the importance of the repeats as "catalytic" domains for microtubule stabilization; one possible interpretation is that phosphorylation disrupts the conformation that is responsible for the strong interaction with tubulin.

Comparison with Previous Studies

Following the discovery of dynamic instability of microtubules by Mitchison and Kirschner (1984), several authors have analyzed it by using video microscopy to observe single microtubules in real time, both in vitro (Horio and Hotani, 1986; Walker *et al.*, 1988; Drechsel *et al.*, 1992; Pryer *et al.*, 1992; Trinczek *et al.*, 1993) or in cells or cell extracts (Cassimeris *et al.*, 1988; Belmont *et al.*, 1990; Verde *et al.*, 1992). It is instructive to compare our results with those of Walker *et al.* (1988) and Drechsel *et al.* (1992). The first of these papers gives a comprehensive description of microtubule dynamics in the absence of MAPs, the second deals more specifically with the influence of tau and its phosphorylation. A comparison of rate constants shows that our data for PC-tubulin are in good agreement with those of Walker *et al.* (compare our Table 1 with their Table 1). For example, at the plus end their dissociation rate is 44 s^{-1} (we find 32 s^{-1}), the critical concentration is 4.9 μM (ours is 4.6 μM), their rate of rapid shortening is 733 s^{-1} (ours is 1138 s^{-1}). Their rescue frequency is about one-half of ours, but in both cases there is only a weak or no dependence on tubulin concentration. The catastrophe frequencies are comparable, and the concentration dependence is relatively weak (in the absence of tau). Given the potential differences in protein preparation and experimental procedures the agreement is quite satisfactory.

Likewise, in the analysis of Drechsel *et al.* (1992) most rate constants and frequencies are also of comparable magnitude (if one allows for variations in experimental procedures); however, there is a striking difference in the dependence of the growth rates on tubulin. The lines pass through the origin, both with or without tau, as if the dissociation rate and critical concentration were essentially zero (cf. their Figure 5a). As a result, the authors have to explain the changes induced by tau largely on the association rate. The absence of a noticeable dissociation rate and critical concentration is at variance with our data, as well as those of Walker *et al.* (1988) and other authors; in our hands, microtubule assembly is always associated with a substantial dissociation rate. It is this parameter, together with the rate of catastrophe, that is mainly affected by tau, and not the association rate constant, which shows little variation. Thus our interpretation echoes that of Murphy *et al.* (1977) who first reported that the effect of MAPs is to reduce dissociation rather than to promote association.

Does this difference in interpretation matter? For most cell biological aspects of microtubules, probably not, but the issue is of interest if one wants to understand the mechanism of microtubule assembly and regulation on a molecular basis. In a simplified view, if tau were to promote microtubule assembly it could be likened to a "match-maker" that actively brings together couples of subunits that otherwise might not meet. If tau were an inhibitor of disassembly it would only act as a "judge of peace", merely sealing bonds that were already made by "couples" of subunits before. This latter view is the one we would favor because it agrees with the observed rate constants.

Another point of debate is the role of phosphorylation. In the report of Drechsel *et al.* (1992), MAP kinase causes a dramatic (15-fold) change in the rate of catastrophe. From our earlier binding studies (Biernat *et al.*, 1993) we had expected that MAP kinase has only a moderate effect, and this is now borne out by the dynamic instability parameters (we compare here the results with those of cdk5 because these two kinases phosphorylate similar sites). The rate of catastrophe changes fourfold, enough to convert tau from strong to medium, but not enough to dissociate it from microtubules. The dramatic change in dynamics (40-fold) is brought about not by the proline-directed phosphorylation, but by the phosphorylation at Ser262 by the kinase MARK (Drewes *et al.*, 1995). This type of phosphorylation converts tau to the weak state, it thus has the potential to dissociate tau from microtubules and cause their breakdown. Interestingly, phosphorylation at Ser-Pro motifs is elevated during mitosis, consistent with higher microtubule dynamics (Preuss *et al.*, 1995), and Ser262 phosphorylation is elevated in Alzheimer tau, and this might be the reason why tau no longer binds to microtubules (Yoshida and Ihara, 1993).

To interpret these results we have to make some seemingly awkward assumptions. The flanking domains are essential for the tight binding of tau to microtubules. These domains are phosphorylated by proline-directed kinases—yet their phosphorylation has only a mild effect on the interaction. On the other hand, the repeats by themselves bind only weakly to microtubules—yet their phosphorylation (at Ser262) abrogates tau's interaction with microtubules. The explanation must lie in the three-dimensional folding of the tau chain, which is not known so far. However, we can summarize the results by stating that the phosphorylation of the targeting domains (flanking regions) has a modulating influence on microbule dy-

namic instability, while phosphorylation of the Ser262 in the catalytic domain (repeats) completely poisons the tau-microtubule interaction. The modulation of the interaction by MAP kinase, cdk5, or others is roughly equivalent to the difference between juvenile 3-repeat tau and adult 4-repeat tau–it matters for processes such as neurite outgrowth or stabilization (Knops *et al.*, 1991; Lo *et al.*, 1993; Leger *et al.*, 1994), but unlike MARK it does not destroy the interaction of tau with microtubules that might become important in other circumstances. This illustrates that there may be more than one level of regulation of tau-microtubule interactions by phosphorylation.

ACKNOWLEDGMENTS

We thank N. Burmester for excellent technical assistance, H.E. Meyer (University of Bochum) for phosphopeptide sequencing, S. Illenberger for help with phosphopeptide mapping, and G. Drewes for making p110^{MARK} available. This project was supported by the Bundesministerium für Forschung und Technologie and the Deutsche Forschungsgemeinschaft.

REFERENCES

Aizawa, H., Emori, Y., Mori, A., Murofushi, H., Sakai, H., and Suzuki, K. (1991). Functional analyses of the domain structure of microtubule-associated protein-4 (MAP-U). J. Biol. Chem. *266*, 9841–9846.

Andersen, S., Buendia, B., Dominguez, J., Sawyer, A., and Karsenti, E. (1994). Effect on microtubule dynamics of XMAP230, a microtubule-associated protein present in *Xenopus* laevis eggs and dividing cells. J. Cell Biol. *127*, 1289–1299.

Baumann, K., Mandelkow, E.-M., Biernat, J., Piwnica-Worms, H., and Mandelkow, E. (1993). Abnormal Alzheimer-like phosphorylation of tau protein by cyclin-dependent kinases cdk2 and cdk5. FEBS Lett. *336*, 417–424.

Beaudette, K., Lew, J., and Wang, J.H. (1993). Substrate specificity characterization of a cdc2-like protein kinase purified from bovine brain. J. Biol. Chem. *268*, 20825–20830.

Bell, C., Fraser, C., Sale, W., Tang, W.-J., and Gibbons, I.R. (1982). Preparation and purification of dynein. Methods Cell Biol. *24*, 373–397.

Belmont, L.D., Hyman, A.A., Sawin, K.E., and Mitchison, T.J. (1990). Real-time visualization of cell-cycle dependent changes in microtubule dynamics in cytoplasmic extracts. Cell *62*, 579–589.

Biernat, J., Gustke, N., Drewes, G., Mandelkow, E.-M., and Mandelkow, E. (1993). Phosphorylation of serine 262 strongly reduces the binding of tau protein to microtubules: distinction between PHF-like immunoreactivity and microtubule binding. Neuron *11*, 153–163.

Brandt, R., Lee, G., Teplow, D.B., Shalloway, D., and Abdelghany, M. (1994). Differential effect of phosphorylation and substrate modulation on tau's ability to promote microtubule growth and nucleation. J. Biol. Chem. *269*, 11776–11782.

Bre, M.H., and Karsenti, E. (1990). Effects of brain microtubule-associated proteins on microtubule dynamics and the nucleating activity of centrosomes. Cell Motil. Cytoskeleton *15*, 88–98.

Brugg, B., and Matus, A. (1991). Phosphorylation determines the binding of microtubule-associated protein-2 (MAP2) to microtubules in living cells. J. Cell Biol. *114*, 735–743.

Butner, K.A., and Kirschner, M.W. (1991). Tau-protein binds to microtubules through a flexible array of distributed weak sites. J. Cell Biol. *115*, 717–730.

Cassimeris, L., Pryer, N.K., and Salmon, E.D. (1988). Real-time observations of microtubule instability in living cells. J. Cell Biol. *107*, 2223–2231.

Chapin, S.J., and Bulinski, J.C. (1992). Microtubule stabilization by assembly-promoting microtubule-associated proteins: a repeat performance. Cell Motil. Cytoskeleton *23*, 236–243.

Cleveland, D.W., Hwo, S.-Y., and Kirschner, M.W. (1977). Physical and chemical properties of purified tau factor and the role of tau in microtubule assembly. J. Mol. Biol. *116*, 227–247.

Coffey, R.L., and Purich, D.L. (1995). Noncooperative binding of the MAP-2 microtubule-binding region to microtubules. J. Biol. Chem. *270*, 1035–1040.

Correas, I., Diaznido, J., and Avila, J. (1992). Microtubule-associated protein tau is phosphorylated by protein kinase C on its tubulin binding domain. J. Biol. Chem. *267*, 15721–15728.

Dhamodharan, R., and Wadsworth, P. (1995). Modulation of microtubule dynamic instability in vivo by brain microtubule-associated proteins. J. Cell Sci. *108*, 1679–1689.

Drechsel, D.N., Hyman, A.A., Cobb, M.H., and Kirschner, M.W. (1992). Modulation of the dynamic instability of tubulin assembly by the microtubule-associated protein tau. Mol. Biol. Cell *3*, 1141–1154.

Drewes, G., Lichtenberg-Kraag, B., Döring, F., Mandelkow, E.-M., Biernat, J., Goris, J., Doree, M., and Mandelkow, E. (1992). Mitogen-activated protein (MAP) kinase transforms tau protein into an Alzheimer-like state. EMBO J. *11*, 2131–2138.

Drewes, G., Trinczek, B., Illenberger, S., Biernat, J., Schmitt-Ulms, G., Meyer, H.E., Mandelkow, E.-M., and Mandelkow, E. (1995). MAP/microtubule affinity-regulating kinase (p110/mark): a novel protein kinase that regulates tau-microtubule interactions and dynamic instability by phosphorylation at the Alzheimer-specific site serine 262. J. Biol. Chem. *270*, 7679–7688.

Ennulat, D.J., Liem, R.K.H., Hashim, G.A., and Shelanski, M.L. (1989). Two separate 18-amino acid domains of tau promote the polymerization of tubulin. J. Biol. Chem. *264*, 5327–5330.

Geisler, N., Heimburg, T., Schünemann, J., and Weber, K. (1993). Peptides from the conserved ends of the rod domain of desmin disassemble intermediate filaments and reveal unexpected structural features: a circular-dichroism, fourier-transform infrared, and electron-microscopic study. J. Struct. Biol. *110*, 205–214.

Gildersleeve, R., Cross, A., Cullen, K., Fagen, A., and Williams, R.C. (1992). Microtubules grow and shorten at intrinsically variable rates. J. Biol. Chem. *267*, 7995–8006.

Goedert, M., Spillantini, M., Jakes, R., Rutherford, D., and Crowther, R.A. (1989). Multiple isoforms of human microtubule-associated protein-tau: sequences and localization in neurofibrillary tangles of Alzheimer's disease. Neuron *3*, 519–526.

Goode, B.L., and Feinstein, S.C. (1994). Identification of a novel microtubule binding and assembly domain in the developmentally regulated inter-repeat region of tau. J. Cell Biol. *124*, 769–782.

Gross, U., Mandelkow, E.-M., Biernat, J., Marx, A., Thiemann, A., Meyer, H.E., Metzger, J., and Mandelkow, E. (1994). Phosphorylation sites in tau protein and paired helical filaments. Mol. Biol. Cell *5*, 289a.

Gustke, N., Trinczek, B., Biernat, J., Mandelkow, E.-M., and Mandelkow, E. (1994). Domains of tau protein and interactions with microtubules. Biochemistry *33*, 9511–9522.

Hanger, D., Hughes, K., Woodgett, J., Brion, J., and Anderton, B. (1992). Glycogen-synthase kinase-3 induces Alzheimer's disease-

like phosphorylation of tau: generation of paired helical filament epitopes and neuronal localization of the kinase. Neurosci. Lett. *147*, 58–62.

Hasegawa, M., Morishima-Kawashima, M., Takio, K., Suzuki, M., Titani, K., and Ihara, Y. (1992). Protein sequence and mass spectrometric analyses of tau in the Alzheimer's disease brain. J. Biol. Chem. *267*, 17047–17054.

Hirokawa, N. (1994). Microtubule organization and dynamics dependent on microtubule-associated proteins. Curr. Opin. Cell Biol. *6*, 74–81.

Horio, T., and Hotani, H. (1986). Visualization of the dynamic instability of individual microtubules by dark-field microscopy. Nature *321*, 605–607.

Ishiguro, K., Omori, A., Sato, K., Tomizawa, K., Imahori, K., and Uchida, T. (1991). A serine threonine proline kinase-activity is included in the tau-protein kinase fraction forming a paired helical filament epitope. Neurosci. Lett. *128*, 195–198.

Itoh, T.J., and Hotani, H. (1994). Microtubule-stabilizing activity of microtubule-associated proteins (MAPs) is due to increase in frequency of rescue in dynamic instability: shortening length decreases with binding of MAPs onto microtubules. Cell Struct. Funct. *19*, 279–290.

Joly, J.C., Flynn, G., and Purich, D.L. (1989). The microtubule-binding fragment of microtubule-associated protein 2: location of the protease-accessible site and identification of an assembly-promoting peptide. J. Cell Biol. *109*, 2289–2294.

Kanai, Y., Chen, J., and Hirokawa, N. (1992). Microtubule bundling by tau proteins in vivo: analysis of functional domains. EMBO J. *11*, 3953–3961.

Knops, J., Kosik, K., Lee, G., Pardee, J., Cohengould, L., and McConlogue, L. (1991). Overexpression of tau in a nonneuronal cell induces long cellular processes. J. Cell Biol. *114*, 725–733.

Kobayashi, S., Ishiguro, K., Omori, A., Takamatsu, M., Arioka, M., Imahori, K., and Uchida, T. (1993). A cdc2-related kinase PSSALRE/cdk5 is homologous with the 30-kDa subunit of tau protein kinase-ii, a proline-directed protein-kinase associated with microtubule. FEBS Lett. *335*, 171–175.

Kosik, K.S., and McConlogue, L. (1994). Microtubule-associated protein function: lessons from expression in *Spodoptera frugiperda* cells. Cell Motil. Cytoskeleton *28*, 195–198.

Kosik, K.S., and Greenberg, S.M. (1994). Tau protein and Alzheimer disease. In: Alzheimer Disease, ed. R. Terry, R. Katzman, and K. Bick, New York: Raven Press, 335–344.

Kowalski, R.J., and Williams, R.C. (1993). Microtubule-associated protein 2 alters the dynamic properties of microtubule assembly and disassembly. J. Biol. Chem. *268*, 9847–9855.

Ledesma, M.D., Correas, I., Avila, J., and Diaz-Nido, J. (1992). Implication of brain cdc2 and MAP2 kinases in the phosphorylation of tau protein in Alzheimer's disease. FEBS Lett. *308*, 218–224.

Lee, G., and Rook, S. (1992). Expression of tau protein in non-neuronal cells: microtubule binding and stabilization. J. Cell Sci. *102*, 227–237.

Leger, J.G., Brandt, R., and Lee, G. (1994). Identification of tau protein regions required for process formation in PC12 cells. J. Cell Sci. *107*, 3403–3412.

Lichtenberg-Kraag, B., Mandelkow, E.-M., Biernat, J., Steiner, B., Schröter, C., Gustke, N., Meyer, H.E., and Mandelkow, E. (1992). Phosphorylation dependent interaction of neurofilament antibodies with tau protein: epitopes, phosphorylation sites, and relationship with Alzheimer tau. Proc. Natl. Acad. Sci. USA *89*, 5384–5388.

Lo, M.M.S., Fieles, A.W., Norris, T.E., Dargis, P.G., Caputo, C.B., Scott, C.W., Lee, V.M.Y., and Goedert, M. (1993). Human tau isoforms confer distinct morphological and functional properties to stably transfected fibroblasts. Mol. Brain Res. *20*, 209–220.

Mandelkow, E.-M., Drewes, G., Biernat, J., Gustke, N., Van Lint, J., Vandenheede, J.R., and Mandelkow, E. (1992). Glycogen synthase kinase-3 and the Alzheimer-like state of microtubule-associated protein tau. FEBS Lett. *314*, 315–321.

Mandelkow, E.-M., and Mandelkow, E. (1993). Tau as a marker for Alzheimer's disease. Trends Biol. Sci. *18*, 480–483.

Meyer, H.E., Hoffmann-Posorske, E., and Heilmeyer, L.M.G. (1991). Determination and location of phosphoserine in proteins and peptides by conversion to *S*-ethyl-cysteine. Methods Enzymol. *201*, 169–185.

Mitchison, T., and Kirschner, M. (1984). Dynamic instability of microtubule growth. Nature *312*, 237–242.

Murphy, D.B., Johnson, K.A., and Borisy, G.G. (1977). Role of tubulin-associated proteins in microtubule nucleation and elongation. J. Mol. Biol. *117*, 33–52.

Obar, R.A., Dingus, J., Bayley, H., and Vallee, R.B. (1989). The RII subunit of cAMP-dependent protein-kinase binds to a common amino-terminal domain in microtubule-associated proteins 2a, 2b, and 2c. Neuron *3*, 639–645.

Olson, K.R., McIntosh, J.R., and Olmstedt, J.B. (1995). Analysis of MAP4 function in living cells using green fluorescent protein (GFP) chimeras. J. Cell Biol. *130*, 639–650.

Ookata, K., Hisanaga, S., Bulinski, J.C., Murofushi, H., Aizawa, H., Itoh, T.J., Hotani, H., Okumura, E., Tachibana, K., and Kishimoto, T. (1995). Cyclin-B interaction with microtubule-associated protein-4 (MAP4) targets p34(cdc2) kinase to microtubules and is a potential regulator of M-phase microtubule dynamics. J. Cell Biol. *128*, 849–862.

Paudel, H., Lew, J., Ali, Z., and Wang, J. (1993). Brain proline-directed protein kinase phosphorylates tau on sites that are abnormally phosphorylated in tau associated with Alzheimer's paired helical filaments. J. Biol. Chem. *268*, 23512–23518.

Preuss, U., Döring, F., Illenberger, S., Mandelkow, E.-M. (1995). Cell cycle dependent phosphorylation and microtubule binding of tau protein stably transfected into Chinese hamster ovary cells. Mol. Biol. Cell *6*, 1397–1410.

Pryer, N., Walker, R., Skeen, V., Bourns, B., Soboeiro, M., and Salmon, E.D. (1992). Brain microtubule-associated proteins modulate microtubule dynamic instability in vitro: real-time observations using video microscopy. J. Cell Sci. *103*, 965–976.

Sammak, P., and Borisy, G. (1988). Direct observation of microtubule dynamics in living cells. Nature *332*, 724–726.

Schoenfeld, T.A., and Obar, R.A. (1994). Diverse distribution and function of fibrous microtubule-associated proteins in the nervous system. Int. Rev. Cytol. *151*, 67–137.

Schulze, E., and Kirschner, M. (1988). New features of microtubule behavior observed in vivo. Nature *334*, 356–359.

Schweers, O., Schönbrunn, E., Marx, A., and Mandelkow, E. (1994). Structural studies of tau protein and Alzheimer paired helical filaments show no evidence for beta structure. J. Biol. Chem. *269*, 24290–24297.

Schweers, O., Mandelkow, E.-M., Biernat, J., and Mandelkow, E. (1995). Oxidation of cysteine 322 in the repeat domain of microtubule-associated protein tau controls the assembly of Alzheimer paired helical filaments. Proc. Natl. Acad. Sci. USA *92*, 8463–8467.

Scott, C., Spreen, R., Herman, J., Chow, F., Davison, M., Young, J., and Caputo, C. (1993). Phosphorylation of recombinant tau by cAMP-dependent protein kinase: identification of phosphorylation sites and effect on microtubule assembly. J. Biol. Chem. *268*, 1166–1173.

Shelden, E., and Wadsworth, P. (1993). Observation and quantification of individual microtubule behavior in vivo: microtubule dynamics are cell-type specific. J. Cell Biol. *120*, 935–945.

Smith, P., Krohn, I., Hermanson, G., Mallia, A., Gartner, F., Provenzano, M., Fujimoto, E., Goeke, N., Olson, B., and Klenk, D. (1985). Measurement of protein using bicinchoninic acid. Anal. Biochem. *150*, 76–85.

Steiner, B., Mandelkow, E.-M., Biernat, J., Gustke, N., Meyer, H.E., Schmidt, B., Mieskes, G., Söling, H.D., Drechsel, D., Kirschner, M.W., Goedert, M., and Mandelkow, E. (1990). Phosphorylation of microtubule-associated protein tau: identification of the site for Ca++-calmodulin-dependent kinase and relationship with tau phosphorylation in Alzheimer tangles. EMBO J. *9*, 3539–3544.

Studier, W.F., Rosenberg, A.H., Dunn, J.J., and Dubendorff, J.W. (1990). Use of T7 RNA polymerase to direct the expression of cloned genes. Methods Enzymol. *185*, 60–89.

Toso, R.J., Jordan, M.A., Farrell, K.W., Matsumoto, B., and Wilson, L. (1993). Kinetic stabilization of microtubule dynamic instability in vitro by vinblastine. Biochemistry *32*, 1285–1293.

Trinczek, B., Marx, A., Mandelkow, E.-M., Murphy, D.B., and Mandelkow, E. (1993). Dynamics of microtubules from erythrocyte marginal bands. Mol. Biol. Cell *4*, 323–335.

Vandecandelaere, A., Martin, S.R., and Bayley, P.M. (1995). Regulation of microtubule dynamic instability by tubulin-GDP. Biochemistry *34*, 1332–1343.

Verde, F., Dogterom, M., Stelzer, E., Karsenti, E., and Leibler, S. (1992). Control of microtubule dynamics and length by cyclin A-dependent and cyclin B-dependent kinases in *Xenopus* egg extracts. J. Cell Biol. *118*, 1097–1108.

Vulliet, R., Halloran, S., Braun, R., Smith, A., and Lee, G. (1992). Proline-directed phosphorylation of human tau protein. J. Biol. Chem. *267*, 22570–22574.

Walker, R., O'Brien, E., Pryer, N., Soboeiro, M., Voter, W., Erickson, H., and Salmon, E. (1988). Dynamic instability of individual microtubules analyzed by video light microscopy: rate constants and transition frequencies. J. Cell Biol. *107*, 1437–1448.

Yoshida, H., and Ihara, Y. (1993). Tau in paired helical filaments is functionally distinct from fetal tau: assembly incompetence of paired helical filament tau. J. Neurochem. *61*, 1183–1186.